Supporting Information

Uriu et al. 10.1073/pnas.0907122107

SI Text

Effects of Random Cell Movement in Lewis's Model (1). We examined the effect of random cell movement on the dynamics of the segmentation clock in Lewis's model (1). We modeled the posterior presomitic mesoderm (PSM) by a 25×10 lattice as in the main text and considered the exchange of location with neighboring cells, which occurs at random time. We assumed that when a cell arrives at a new location it immediately begins interacting with its new neighbors through Delta–Notch signaling and immediately stops interacting with its old neighbors.

Each cell in the lattice is identified by index j ($j = 1, 2, \ldots..., N$). Let $m_{\mathrm{h1}}^{(j)}(t)$, $m_{\mathrm{h7}}^{(j)}(t)$, $m_{\mathrm{d}}^{(j)}(t)$ be the number of *her*1, *her*7, and *delta* mRNA copies in cell j, respectively. Let $p_{\mathrm{H1}}^{(j)}(t)$, $p_{\mathrm{H7}}^{(j)}(t)$, $p_{\mathrm{D}}^{(j)}(t)$ be the number of Her1, Her7, and Delta protein copies in cell j, respectively. In Lewis's model, the dynamics of these variables is given as follows:

$$\frac{dm_{\mathrm{h1}}^{(j)}(t)}{dt} = \frac{k\{1+\bar{\phi}_{\mathrm{D}}^{(j)}(t-T_{\mathrm{h1}})\}}{1+\bar{\phi}_{\mathrm{D}}^{(j)}(t-T_{\mathrm{h1}})+\phi_{\mathrm{H1}}^{(j)}(t-T_{\mathrm{h1}})\phi_{\mathrm{H7}}^{(j)}(t-T_{\mathrm{h1}})} - c_{\mathrm{h1}}m_{\mathrm{h1}}^{(j)}(t) \qquad \textbf{[S1a]}$$

$$\frac{dm_{\mathrm{h7}}^{(j)}(t)}{dt} = \frac{k\{1+\bar{\phi}_{\mathrm{D}}^{(j)}(t-T_{\mathrm{h7}})\}}{1+\bar{\phi}_{\mathrm{D}}^{(j)}(t-T_{\mathrm{h7}})+\phi_{\mathrm{H1}}^{(j)}(t-T_{\mathrm{h7}})\phi_{\mathrm{H7}}^{(j)}(t-T_{\mathrm{h7}})} - c_{\mathrm{h7}}m_{\mathrm{h7}}^{(j)}(t) \qquad \textbf{[S1b]}$$

$$\frac{dm_{\mathrm{d}}^{(j)}(t)}{dt} = \frac{k}{1+\phi_{\mathrm{H1}}^{(j)}(t-T_{\mathrm{d}})\phi_{\mathrm{H7}}^{(j)}(t-T_{\mathrm{d}})} - c_{\mathrm{d}}m_{\mathrm{d}}^{(j)}(t) \qquad \textbf{[S1c]}$$

$$\frac{dp_{\mathrm{H1}}^{(j)}(t)}{dt} = am_{\mathrm{h1}}^{(j)}(t-T_{\mathrm{H1}}) - b_{\mathrm{H1}}p_{\mathrm{H1}}^{(j)}(t) \qquad \textbf{[S1d]}$$

$$\frac{dp_{\mathrm{H7}}^{(j)}(t)}{dt} = am_{\mathrm{h7}}^{(j)}(t-T_{\mathrm{H7}}) - b_{\mathrm{H7}}p_{\mathrm{H7}}^{(j)}(t) \qquad \textbf{[S1e]}$$

$$\frac{dp_{\mathrm{D}}^{(j)}(t)}{dt} = am_{\mathrm{d}}^{(j)}(t-T_{\mathrm{D}}) - b_{\mathrm{D}}p_{\mathrm{D}}^{(j)}(t) \qquad \textbf{[S1f]}$$

where $\phi_{\mathrm{H1}}^{(j)}(t) = p_{\mathrm{H1}}^{(j)}(t)/p_{0\mathrm{H}}$, $\phi_{\mathrm{H7}}^{(j)}(t) = p_{\mathrm{H7}}^{(j)}(t)/p_{0\mathrm{H}}$, and $\bar{\phi}_{\mathrm{D}}^{(j)}(t) = \bar{p}_{\mathrm{D}}^{(j)}(t)/p_{0\mathrm{D}}$. T_{ξ} ($\xi = \mathrm{h1}, \mathrm{h7}, \mathrm{d}, \mathrm{H1}, \mathrm{H7}, \mathrm{D}$) represents a time delay caused by the modification and the transport of molecules.

Eqs. **S1a** and **S1b** represent the time evolution of *her*1 and *her*7 mRNA, respectively. The first term of these two equations represents the transcription of mRNA. Lewis (1) assumed that Her1 and Her7 protein form a dimmer, then it suppresses the transcription of *her*1 and *her*7 mRNA. In Lewis's model, a two-cell coupling system was analyzed. Extending his model to a two-dimensional model, we assumed that each cell receives Delta–Notch signaling from its four nearest neighbors; $\bar{p}_{\mathrm{D}}^{(j)}(t)$ [$\bar{p}_{\mathrm{D}}^{(j)}(t) = p_{0\mathrm{D}}\bar{\phi}_{\mathrm{D}}^{(j)}(t)$] in Eqs. **S1a** and **S1b** is the average of Delta protein amount over four neighboring cells (2). For cells on the boundaries, $\bar{p}_{\mathrm{D}}^{(j)}(t)$ is the average of two or three neighbors. The second term of these equations represents the degradation of *her*1 and *her*7 mRNA molecules. Eq. **S1c** describes the time evolution of *delta* mRNA. Her1/7 dimmers suppress the transcription of *delta* mRNA (the first term). The second term represents the degradation of *delta* mRNA molecules.

Eqs. **S1d**, **S1e**, and **S1f** represent the time evolution of Her1, Her7, and Delta protein, respectively. The first term of these equations represents the production of proteins by translation and the second term represents the degradation of proteins.

For the numerical calculations of the model, we used the same reaction parameters as in Ozbudak and Lewis (3) as a standard parameter set: $a = 4.5$, $b_{\mathrm{H1}} = b_{\mathrm{H7}} = b_{\mathrm{D}} = 0.23$, $c_{\mathrm{h1}} = 0.253$, $c_{\mathrm{h7}} = 0.206$, $c_{\mathrm{d}} = 0.273$, $k = 33\ \mathrm{min}^{-1}$; $p_{0\mathrm{H}} = 40$, $p_{0\mathrm{D}} = 400$; $T_{\mathrm{h1}} = 7.8$, $T_{\mathrm{h7}} = 7.7$, $T_{\mathrm{d}} = 12.4$, $T_{\mathrm{H1}} = 2.8$, $T_{\mathrm{H7}} = 1.7$, $T_{\mathrm{D}} = 20.5\,\mathrm{min}$. With the standard parameter set, the period of synchronized oscillation was 38.47 min.

To study the effect of random cell movement on the dynamics of the segmentation clock, we examined how global synchronization is recovered against an external perturbation as in the main text. First we defined the phase (θ) on the limit cycle with all N cells perfectly synchronized. The value of phase ranged from 0 to 2π and became zero when the amount of *her*1 mRNA was maximal. Then, an initial phase randomly chosen from within the interval $[-2\pi(\alpha/2), 2\pi(\alpha/2)]$ was allotted to each cell, where α is a parameter controlling the magnitude of the initial phase difference between cells. Each variable for each cell at time τ ($-T_{\mathrm{D}} \leq \tau < 0$) was set to the value corresponding to the phase on the limit cycle [i.e., $\theta(t=0) + 2\pi\tau/T_p$] where T_p is the period of the limit cycle.

We confirmed that random cell movement shortened the time taken to recover global synchronization against the initial phase differences between cells (Fig. S1), that it expanded the parameter range that allows global synchronization to be achieved (Fig. S2), and that there was an optimal magnitude of anisotropy in the direction of cell movement that depends on the aspect ratio of the lattice (Fig. S3).

Effects of Random Cell Movement in an Abstract Phase Dynamics Model. Next we examined the effect of random cell movement in an abstract phase dynamics model; concretely, we adopted a model proposed by Sakaguchi et al. (4) whose dynamics has been often studied in physics. As shown below, the results shown in the main text and in the last section hold even if we model the segmentation clock by the abstract phase dynamics model.

Let $\theta_j(t)$ be the phase of oscillation of the segmentation clock in cell j ($j = 1, 2, \ldots, N$). The value of $\theta_j(t)$ ranges from 0 to 2π. The time evolution of $\theta_j(t)$ is given by

$$\frac{d\theta_j}{dt} = \omega_j + K\sum_{<\alpha>}\sin(\theta_\alpha - \theta_j) + \xi_j(t), \qquad \textbf{[S2]}$$

where ω_j is the speed of phase advance (natural frequency) of the segmentation clock in cell j, K is the coupling strength between two cells, and $\xi_j(t)$ is the white Gaussian noise with zero mean and correlations, $\langle \xi_j(t)\xi_k(t')\rangle = \sigma_\xi^2\delta(t-t')\delta_{jk}$. We assumed that the natural frequency has cell-to-cell variability and the variability was modeled by a normal distribution $N(\bar{\omega}, \sigma_\omega^2)$ where $\bar{\omega}$ represents the population average and σ_ω^2 represents the variance. $\sum_{<\alpha>}$ in Eq. **S2** represents the summation over all the nearest neighbors of cell j.

We adopted a 25×10 lattice ($N = 250$). We set $\bar{\omega} = 0.21\ \mathrm{min}^{-1}$ so that the population average of period ($2\pi/\bar{\omega}$) was 30 min. (Fig. S4*J*–*L*). We set $K = 0.0175\ \mathrm{min}^{-1}$ based on the estimation of coupling strength between two oscillators by

Riedel-Kruse et al. (5). We treated σ_ξ and σ_ω as free parameters (Fig. S4*A*–*I*). The initial phase of each cell $[\theta_j(0)]$ was chosen randomly from a uniform distribution between $-\pi$ to π (i.e., $\alpha = 1.0$).

To quantify the degree of phase synchrony, we used an order parameter $re^{i\psi} = \frac{1}{N}\sum_{j=1}^{N} e^{i\theta_j}$, where $i = \sqrt{-1}$ (6). The radius r measures the magnitude of phase synchronization and ψ represents the average phase over N cells. In the synchronized state, $r \approx 1$, whereas $r \approx 0$ in unsynchronized states. We confirmed that random cell movement promotes synchronization of the segmentation clock even in the presence of noises and the cell-to-cell variability in the natural frequency (Fig. S4*A*–*I*).

Model in Which Cells Need Several Minutes to Efficiently Interact with Their Neighbors After an Exchange of Locations. In the main text, we assumed that when a cell arrives at a new location it immediately interacts with its new neighbors. Here we study the model in which each cell needs several minutes to efficiently interact with its new neighbors after an exchange of location in order to demonstrate that cell movement facilitates the synchronization of the segmentation clock even under such a situation.

We consider the binding ability of each cell to its neighboring cells with Delta and Notch proteins. Let the binding ability be represented as a value between zero and one (larger value represents higher binding ability). The binding ability of cell j is denoted by c_j ($j = 1, 2, \ldots, N$). We assume that when a cell changes the location, its binding ability is zero (i.e., the cell is unable to interact with its new neighbors right after the exchange of the location) and that it recovers after the last exchange of location according to the following equation:

$$c_j(\tau) = 1 - e^{-\beta\tau}, \qquad \textbf{[S3]}$$

where τ is the elapsed time after the last exchange of location for cell j, β is the positive constant and determines the recovery speed of binding ability (see Fig. S6*A*).

In Eq. **2a** in *Appendix* we assume that Delta–Notch signaling received from neighboring cells ($\hat{w}_j$) is the average of the Delta protein concentrations over the four neighboring cells. We redefine $\hat{w}_j$ in Eq. **2a** using the binding availability. Let c_j^{left}, c_j^{right}, c_j^{up}, and c_j^{down} be the binding ability of left, right, up, and down neighbors of cell j, respectively. Let τ_{left}, τ_{right}, τ_{up}, and τ_{down} be the elapsed time after the last exchange of locations for left, right, up, and down neighbors of cell j, respectively. We redefine $\hat{w}_j$ in Eq. **2a** as follows:

$$\begin{aligned}\hat{w}_j = c_j(\tau)\{&c_j^{\text{left}}(\tau_{\text{left}})w_j^{\text{left}} + c_j^{\text{right}}(\tau_{\text{right}})w_j^{\text{right}} + c_j^{\text{up}}(\tau_{\text{up}})w_j^{\text{up}} \\ &+ c_j^{\text{down}}(\tau_{\text{down}})w_j^{\text{down}}\}/[c_j^{\text{left}}(\tau_{\text{left}}) + c_j^{\text{right}}(\tau_{\text{right}}) \\ &+ c_j^{\text{up}}(\tau_{\text{up}}) + c_j^{\text{down}}(\tau_{\text{down}})],\end{aligned} \qquad \textbf{[S4]}$$

where w_j^{left}, w_j^{right}, w_j^{up}, and w_j^{down} are the Delta protein concentrations expressed by left, right, up, and down neighbors of cell j, respectively.

Fig. S6*B* shows the average time course of *IS* when each cell experienced an exchange of location within 10 min on average (red filled circles, green open circles, and blue filled squares) and when cells did not move (pink open squares). The magnitude of the initial phase differences was set to $\alpha = 0.6$ in Fig. S6*B*. When the binding ability of each cell recovered in about 1 min (red filled circles), cells could restore the synchronization faster than when they did not move. When cells needed about 2 or 3 min to recover their binding ability after an exchange of location (green open circles and blue filled squares, respectively), *IS* converged to the values smaller than one. However, cells could sustain highly synchronized state (*IS* ≈ 0.9 even for the 3 min case).

Fig. S6*C* shows the average time course of *IS* when the magnitude of the initial phase differences was set to $\alpha = 1.0$. Even when cells needed 3 min for full recovery of binding ability, they rapidly reached to highly synchronized states. In contrast, when cells did not move, *IS* slowly increased and at last after 40 cycles they caught up with *IS* value of cells exchanging their locations. Hence, we concluded that cell movement enables cells to rapidly reach synchronized states even under a penalty for it.

1. Lewis J (2003) Autoinhibition with transcriptional delay: A simple mechanism for the zebrafish somitogenesis oscillator. *Curr Biol* 13:1398–1408.
2. Tiedemann HB et al. (2007) Cell-based simulation of dynamic expression patterns in the presomitic mesoderm. *J Theor Biol* 248:120–129.
3. Ozbudak EM, Lewis J (2008) Notch signalling synchronizes the zebrafish segmentation clock but is not needed to create somite boundaries. *PLoS Genet* 4:e15.
4. Sakaguchi H, Shinomoto S, Kuramoto Y (1987) Local and global self-entrainments in oscillator lattices. *Prog Theor Phys* 77:1005–1010.
5. Riedel-Kruse IH, Muller C, Oates AC (2007) Synchrony dynamics during initiation, failure, and rescue of the segmentation clock. *Science* 317:1911–1915.
6. Kuramoto Y (1984) *Chemical oscillations, waves, and turbulence* (Springer–Verlag, Berlin).

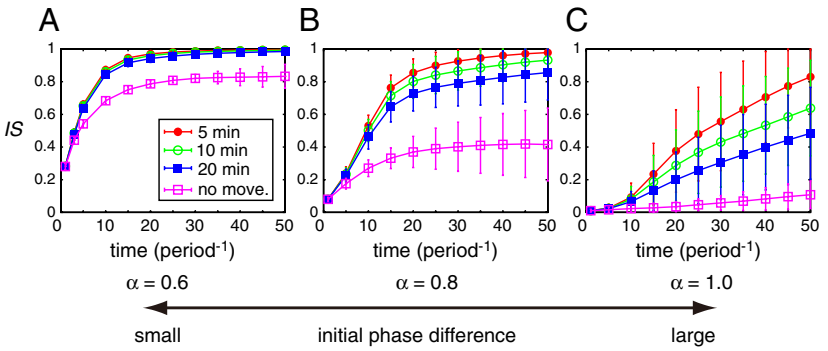

Fig. S1. Random cell movement facilitates the synchronization of the segmentation clock in Lewis's model given by Eq. **S1a**–**S1f**. (*A*–*C*) Average time course of *IS* when the magnitude of the initial phase differences between cells was set to (*A*) $\alpha = 0.6$, (*B*) $\alpha = 0.8$, and (*C*) $\alpha = 1.0$. Each cell experienced an exchange of its location with one of its neighbors within 5 min (red filled circles), 10 min (green open circles), or 20 min (blue filled squares) on average. Pink open squares represent the case in which all *N* cells were fixed in the lattice. We used 10 different initial conditions. We ran 50 simulations for each initial condition when we considered cell movement. We averaged all of the trials (500 runs for the systems with cell movement and 10 runs for the system with cells fixed in the lattice). Error bars indicate SD. Reaction parameters used in Eq. **S1a**–**S1f** are listed in the first paragraph of *SI Text*.

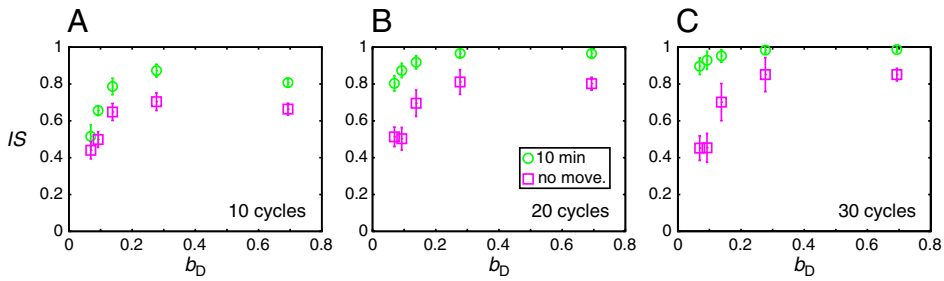

Fig. S2. Cell movement extends the parameter range that allows cells to achieve synchronization in Lewis's model given by Eq. **S1a**–**S1f**. (*A*–*C*) The average *IS* for different values of the degradation rate of Delta protein (b_D) (*A*) after 10 cycles, (*B*) 20 cycles, and (*C*) 30 cycles. Each cell experienced an exchange of its location with one of its neighbors within 10 min on average (green circles). Pink open squares represent the case in which all *N* cells were fixed in the lattice. Other parameters were set to the standard values listed in in the first paragraph of *SI Text*. The magnitude of the initial phase differences between cells was set to $\alpha = 0.6$. We used five different initial conditions for each b_D. We ran 50 simulations for each initial condition when we considered cell movement. Then we averaged all trials. Error bars indicate SD.

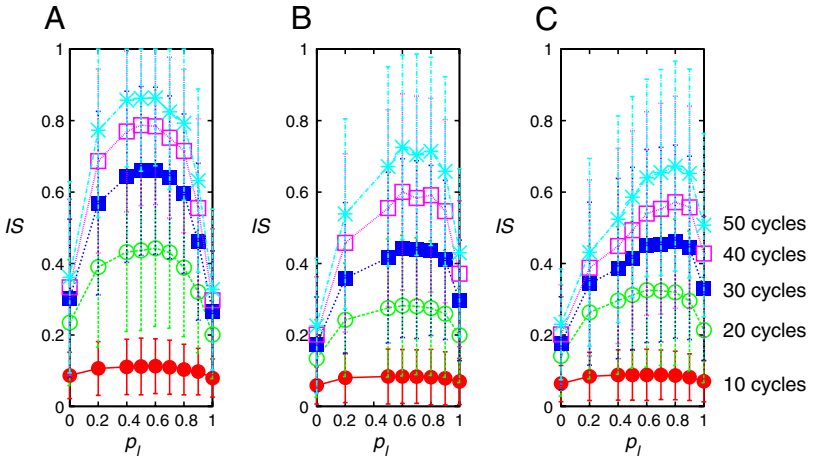

Fig. S3. The optimal magnitude of anisotropy in the direction of cell movement is determined by the aspect ratio of the lattice in Lewis's model given by Eq. **S1a**–**S1f**. (*A*–*C*) Average *IS* was calculated over 500 simulations for different p_l (the probability of the exchange of location in the direction of the long side of the lattice) in (*A*) a 16×16 lattice, (*B*) a 25×10 lattice, and (*C*) a 32×8 lattice. Each cell experienced an exchange of its location with one of its neighbors within 10 min on average. The magnitude of the initial phase differences between cells was set to $\alpha = 1.0$. We used 10 different initial conditions and ran 50 simulations for each initial condition.

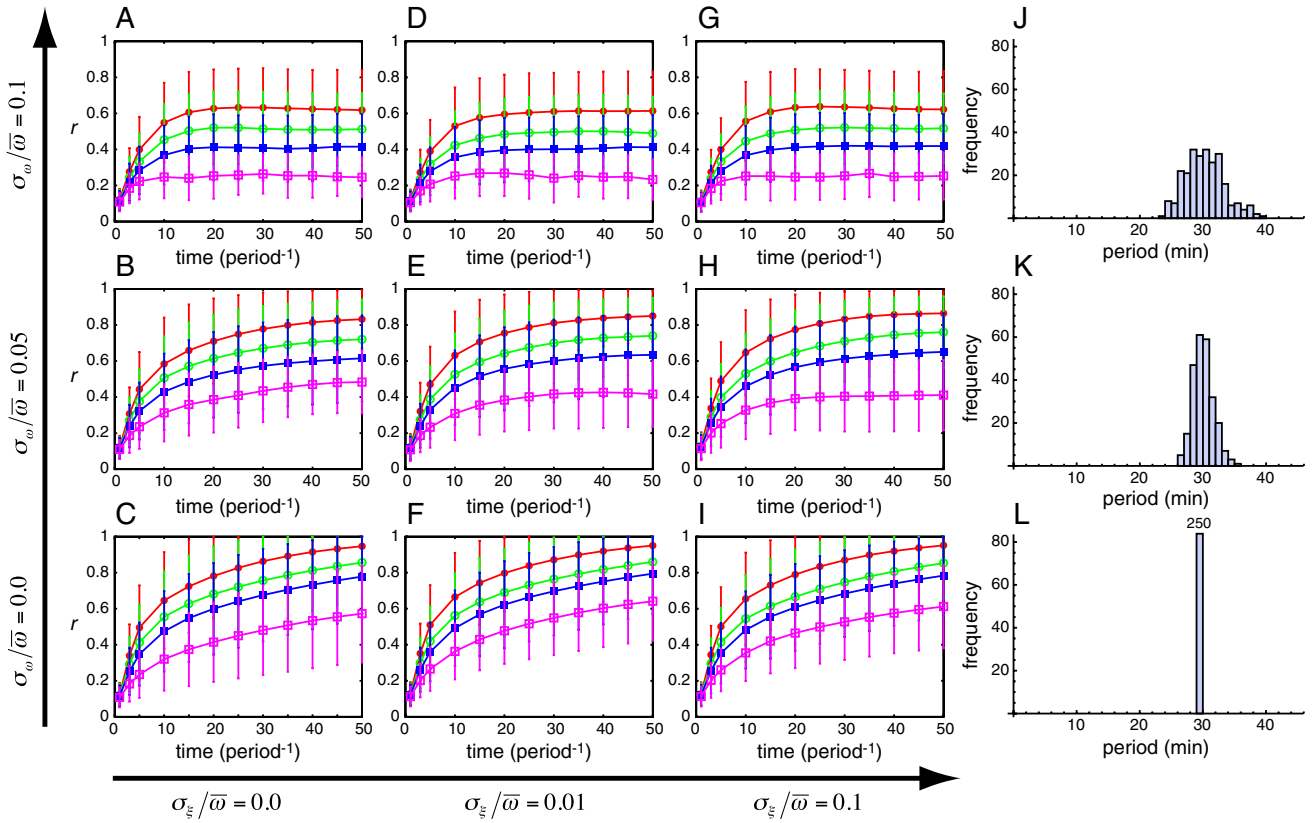

Fig. S4. Cell movement facilitates the synchronization in the phase dynamics model given by Eq. **S2**. (*A–I*) The average time course of order parameter *r* for different pairs of σ_ξ and σ_ω in Eq. **S2**. Each cell experienced an exchange of its location with one of its neighbors within 5 min (red filled circles), 10 min (green open circles), or 20 min (blue filled squares) on average. Pink open squares represent the case in which all *N* cells were fixed in the lattice. In (*A*), (*B*), (*D*), (*E*), (*G*), and (*H*), we generated 10 different distributions of speed of phase advance (natural frequency) among cells and we used 10 different initial conditions for each distribution. In (*C*), (*F*), and (*I*), we used 100 different initial conditions. We ran 10 simulations for each initial condition when we considered cell movement and/or noises (i.e., $\sigma_\xi > 0.0$). We averaged all trials [100 runs for systems with cells fixed in the lattice in (*A–C*), 1,000 runs for the others]. (*J–L*) Examples of the period distribution among cells: (*J*) $\sigma_\omega/\bar{\omega} = 0.1$, (*K*) $\sigma_\omega/\bar{\omega} = 0.05$, and (*L*) $\sigma_\omega/\bar{\omega} = 0.0$ ($\bar{\omega} = 0.21$ min^{-1}). In (*A–I*) error bars indicate SD.

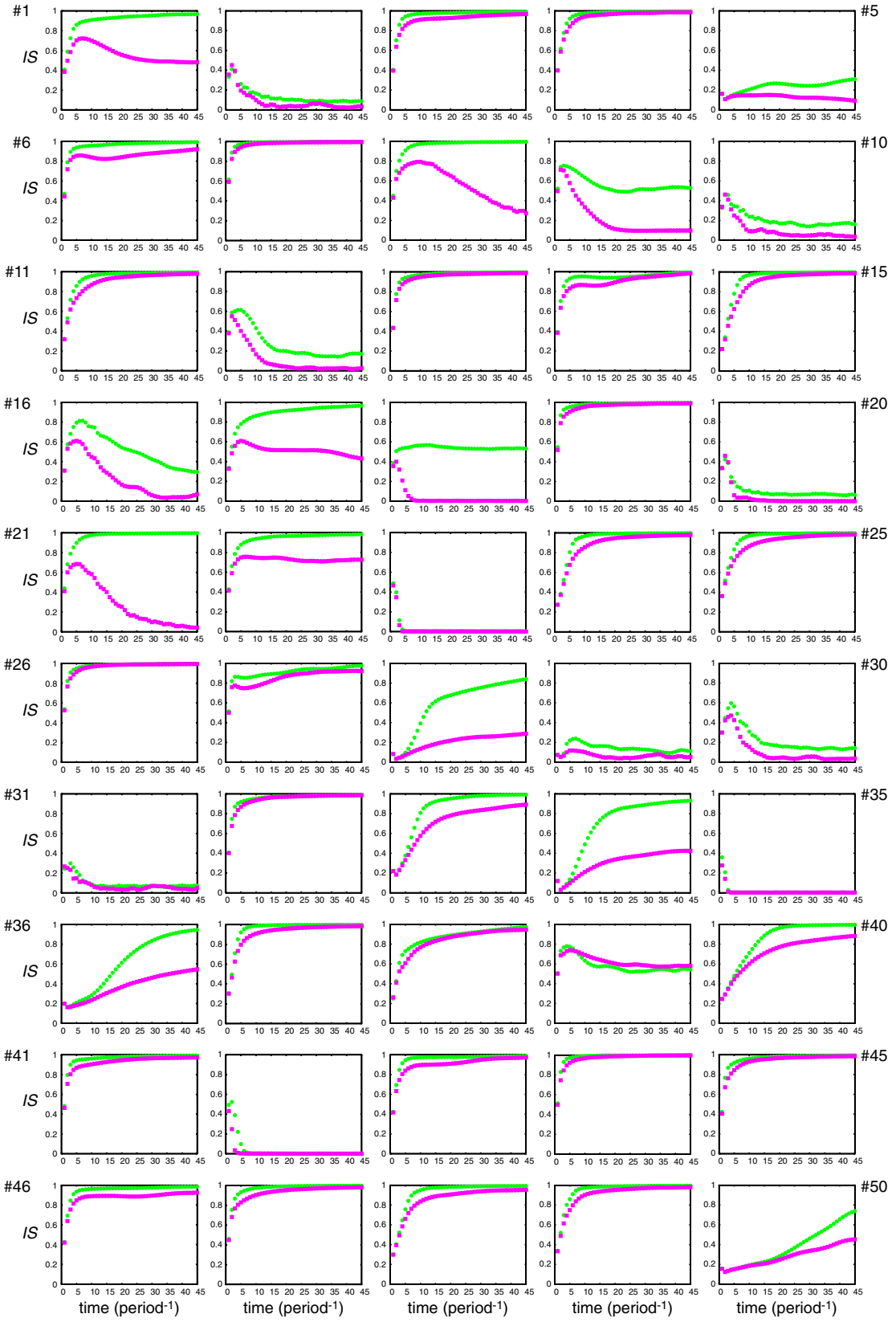

Fig. S5. Random cell movement enhances the restoration of synchronization of the segmentation clock in the wide range of reaction parameters in Eq. **2** in the main text. (#1–#50) Results for 50 different parameter sets. Each cell experienced an exchange of its location with one of its neighbors within 10 min (green circles) on average. Pink squares represent the case in which all *N* cells were fixed in the lattice. The magnitude of the initial phase differences between cells was set to $\alpha = 0.6$. We used 10 different initial conditions for each parameter set. We ran 10 simulations for each initial condition when we considered cell movement. We averaged all trials (100 runs for systems with cell movement and 10 runs for systems with cells fixed in the lattice).

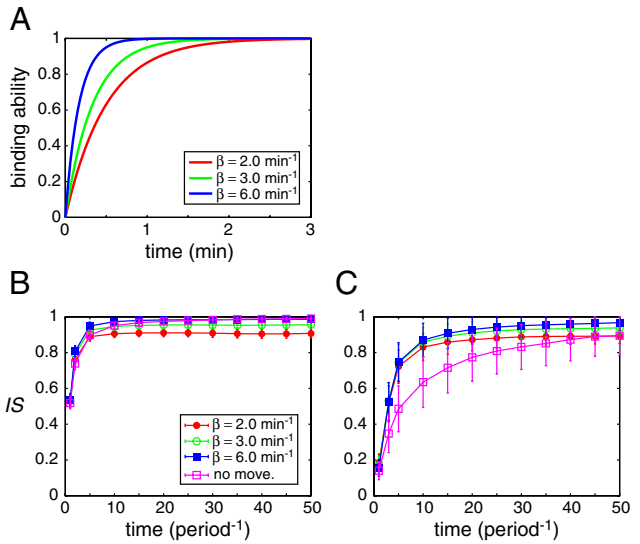

Fig. S6. Random cell movement facilitates the synchronization of the segmentation clock even when each cell needs several minutes to efficiently interact with its new neighbors after an exchange of location. (*A*) Recovery of binding ability under Eq. **S3**. $\beta = 2.0$ min^{-1} (*Red*), 3.0 min^{-1} (*Green*), and 6.0 min^{-1} (*Blue*). (*B*, *C*) The average time course of *IS* when the magnitude of the initial phase differences between cells was set to (*B*) $\alpha = 0.6$ and (*C*) $\alpha = 1.0$. Each cell experienced an exchange of its location with one of its neighbors within 10 min on average. The binding ability of each cell needs about 1 min ($\beta = 6.0$ min^{-1}, blue squares), 2 min ($\beta = 3.0$ min^{-1}, green open circles), and 3 min ($\beta = 2.0$ min^{-1}, red filled circles) for full recovery. Pink open squares represent the case in which all *N* cells were fixed in the lattice. We used 20 different initial conditions. We ran 50 simulations for each initial condition when we considered cell movement. Then we averaged all trials (1,000 runs for systems with cell movement and 20 runs for systems with cells fixed in the lattice). Error bars indicate SD. Reaction parameters used in Eq. **2** are listed in the main text (*Appendix*) as a standard parameter set.

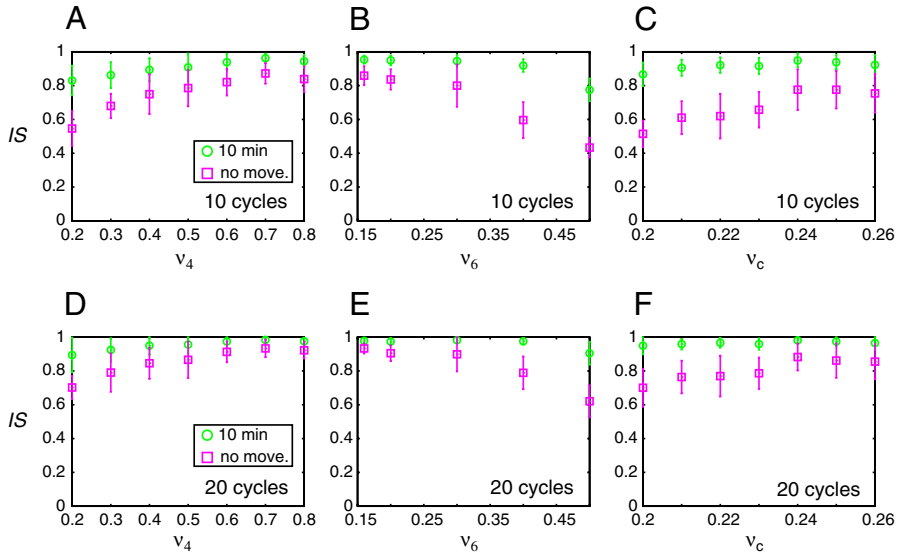

Fig. S7. Expansion of a parameter range where the synchronization is recovered against the perturbation for the initial phase and stably maintained in the presence of random cell movement. (*A*–*C*) The average *IS* for different values of (*A*) the degradation rate of Her protein in cytoplasm (ν_4), (*B*) the degradation rate of Her protein in nucleus (ν_6), and (*C*) the activation rate of *her* mRNA transcription by Delta–Notch signaling (ν_c) after 10 cycles. Green open circles represent the case in which each cell experienced an exchange of its location with one of its neighbors within 10 min on average. Pink open squares represent the case in which cells were fixed in the lattice. In (*A*–*C*) parameters other than focal parameter were set to the standard values listed in the main text (*Appendix*). The magnitude of the initial phase differences between cells was set to $\alpha = 0.8$. We used 10 different initial conditions for each parameter set. We ran 10 simulations for each initial condition when we considered cell movement. We averaged all trials (100 runs for systems with cell movement and 10 runs for systems with cells fixed in the lattice). (*D*–*F*) The average *IS* after 20 cycles. Error bars indicate SD.

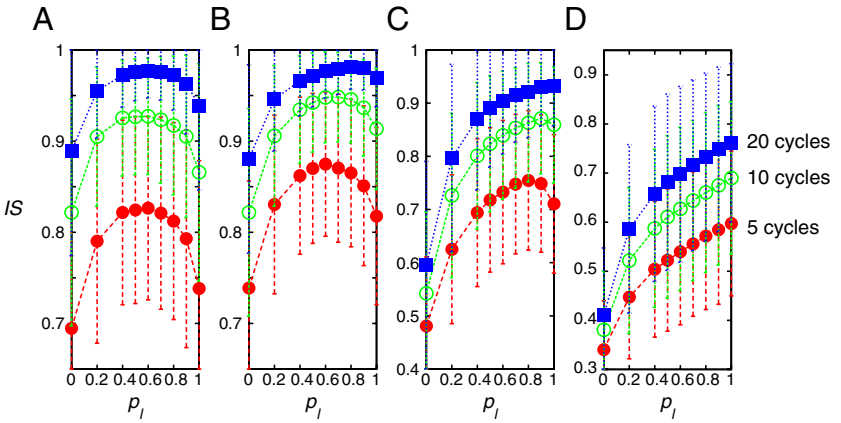

Fig. S8. The optimal magnitude of anisotropy in the direction of cell movement does not depend on the total cell number N and whether the aspect ratio of the lattice is an integer. (*A*–*D*) Average *IS* over 2,000 simulations at 5, 10, and 20 cycles when each cell exchanged its location with its neighbors with each p_l in (*A*) a 20×13 lattice, (*B*) a 28×8 lattice, (*C*) a 50×4 lattice, and (*D*) a 128×2 lattice. In (*A*–*D*), each cell experienced an exchange of its location with one of its neighbors within 5 min on average. The magnitude of the initial phase differences between cells was set to $\alpha = 1.0$. We used 20 different initial conditions. We ran 100 simulations for each initial condition. Error bars indicate SD. Reaction parameters used in Eq. **2** are listed in the main text (*Appendix*) as a standard parameter set.

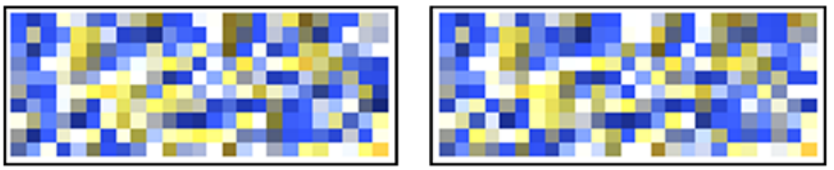

Movie S1. Time evolution of *her* mRNA for 25×10 cells. In the left movie, all cells are fixed in the two-dimensional lattice. In the right movie, each cell experiences an exchange of its location within 10 min on average. Orange (blue) color indicates high (low) *her* mRNA concentration.

Movie S1 (MOV)

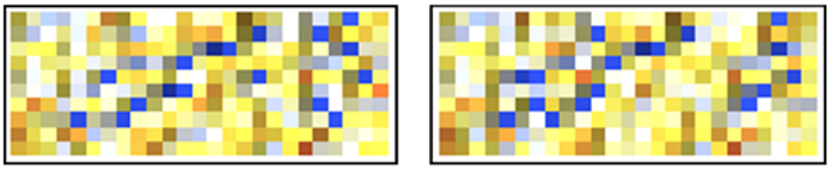

Movie S2 Example of spatiotemporal pattern of *her* gene expression in which an initial synchronized state was not maintained without cell movement. In the left movie, all cells are fixed in the two-dimensional lattice. In the right movie, each cell experiences an exchange of its location within 10 min on average. Orange (*Blue*) color indicates high (low) *her* mRNA concentration.

Movie S2 (MOV)

Table S1. Ranges from which parameters were selected

Parameter	Definition	Range and units
ν_1	Basal transcription rate of *her* mRNA	0.001–0.1 nM min^{-1}
ν_2	Maximum degradation rate of *her* mRNA	0.1–10 nM min^{-1}
ν_3	Translation rate of Her protein	0.5–50 min^{-1}
ν_4	Maximum degradation rate of Her protein in cytoplasm	0.1–10 nM min^{-1}
ν_5	Cytoplasm-nucleus transport rate of Her protein	0.01–1.0 min^{-1}
ν_6	Maximum degradation rate of Her protein in nucleus	0.1–10 nM min^{-1}
ν_7	Synthesis rate of Delta protein	0.1–10 nM min^{-1}
ν_8	Maximum degradation rate of Delta protein	0.1–10 nM min^{-1}
ν_c	Activation rate of *her* mRNA transcription by Delta–Notch signaling	0.01–1.0 min^{-1}
K_1	Threshold constant for the suppression of *her* mRNA by Her protein	0.1–10 nM
K_2	Michaelis constant for *her* mRNA degradation	0.1–10 nM
K_4	Michaelis constant for Her protein degradation in cytoplasm	0.1–10 nM
K_6	Michaelis constant for Her protein degradation in nucleus	0.1–10 nM
K_7	Threshold constant for the suppression of Delta protein by Her protein	0.1–10 nM
K_8	Michaelis constant for Delta protein degradation	0.1–10 nM